

# Experimental Investigations into Electric Discharge Grinding of $\text{Al}_2\text{O}_3\text{-SiC}_w\text{-TiC}$ Ceramic Composite

M. K. Satyarthi

Assistant Professor,

Deptt. Of Mech. And Automation Engg.,

USICT, Guru Gobind Singh Indraprastha University Delhi,  
New Delhi, India – 110078

Dr. Pulak M. Pandey

Associate Professor,

Mech. Engg. Department,

Indian Institute of Technology Delhi,  
New Delhi, India – 110016

**Abstract:** The physical and mechanical properties of ceramic composite materials make their processing difficult by conventional processes. The electric discharge machining (EDM) and conventional grinding processes has been tried successfully in the recent past to machine  $\text{Al}_2\text{O}_3\text{-SiC}_w\text{-TiC}$  ceramic composite. Although the processing of alumina ceramic was successful, the defects induced by processes were also evident. In the present work, electric discharge grinding (EDG) has been tried as an alternative for machining of  $\text{Al}_2\text{O}_3\text{-SiC}_w\text{-TiC}$  ceramic composite. The cost effective utilization of electric discharge grounded components in commercial applications relies on the material removal mechanisms, its relationship with the EDG parameters and the formation of surface and sub-surface damages. Therefore, influence of process factors like discharge current, duty cycle, pulse on time, table speed, and wheel speed has been studied on material removal rate (MRR) and surface roughness (SR). The central composite rotatable design (CCRD) has been used to plan the experiments. Optimization of process factors has been done to obtain the highest MRR and lowest SR. It was found that the contribution of process factors like duty cycle, pulse on time, table speed and wheel speed were significant on MRR. The contribution of discharge current alone in the selected range was found insignificant. It was observed that the MRR achieved was 4 to 10 times higher in EDG than EDM process. The process factors like discharge current, duty cycle, pulse on time and its interactions shows significant contribution on SR, whereas, the contribution of wheel speed and table speed were insignificant. Although the ratios of wheel speed to table speed affects the SR. It has been established that the SR obtained by EDG is less than EDM and conventional diamond grinding processes. It was also observed that the SR obtained is 2 to 5 times lower in EDG than EDM process. The surface and subsurface damages were assessed and characterized by scanning electron microscope (SEM). The surface produced by EDG was found free from surface/sub-surface defects. The recast layer was observed in few cases and was swept uniformly along the work surface resulting in low SR.

**Key words:** *Electric Discharge Grinding, Material Removal Rate, Surface Roughness, Surface Integrity, Conductive Ceramic.*

## INTRODUCTION

Ceramic materials can retain its properties like wear resistance, high hardness, resistance to chemical degradation and low density at elevated temperatures and corrosive environments. These makes ceramics potentially unique solutions for number of engineering applications like aero

engines, automobiles, defence, bio-medical, cutting tool and die manufacturing. The alumina ceramic material shows bio-compatibility [1] therefore it has applications in medical, which includes manufacturing of hip implant [2], dental crown and implant [3]. The improved physical and mechanical properties makes alumina ceramic a suitable candidate for cutting tool inserts [4, 5], turbine blades [6, 7] and armours [8]. Despite of the fact that alumina ceramic in particular is attractive for engineering applications but has not been explored fully to its potentials. This may be due to the difficulties associated with ceramic material processing for intricate shapes without defects or material property alteration.

The widespread applications of alumina ceramic composite has attracted keen interest of researchers [9-15] to develop the cost effective machining process. The improvement in mechanical and electrical properties of the single-phase ceramic materials has been achieved by adding  $\text{SiC}_w$  and electrically conductive phase elements like transition-metals containing carbides, borides and nitrides respectively. The addition of 40%  $\text{TiB}_2$  by volume improved the hardness and fracture toughness, and raised the conductivity so that electric discharge machining (EDM) and hybrid machining processes could be used [16]. Similarly, the reinforcement of conductive phase like TiC particles in  $\text{Al}_2\text{O}_3\text{-SiC}_w$  ceramic raised the electrical conductivity to process the material by EDM. The machining of  $\text{Al}_2\text{O}_3\text{-SiC}_w\text{-TiC}$  ceramic has been successful by EDM, conventional diamond grinding and EDG [9-14, 17-19] in recent past. In the following section a brief literature review has been presented to describe machinability and the effects of process parameters in processing of  $\text{Al}_2\text{O}_3$  based ceramic composites.

## LITERATURE REVIEW

The unconventional machining process like EDM has been realised as one of the prominent process to machine  $\text{Al}_2\text{O}_3\text{-SiC}_w\text{-TiC}$  ceramic. The influence of process parameters and optimization was attempted by few researchers [9-11] and [20] to study responses like material removal rate (MRR), tool wear rate (TWR) and surface integrity. The degradation in strength was noticed in their [9-11, 20] work due to EDM induced damages. The input process parameters like peak current, discharge voltage and pulse on time significantly influenced the MRR [21-23] during EDM processing. It was

also found that the MRR was high for higher discharge energies which promoted areas of thermal spalling due to induced thermal-shock [24]. Thermal shocks detached the surface layers of ceramic material as clusters which resulted in higher MRR at increased pulse on time [24]. It was found that the average recast layer thickness was primarily dependent on discharge current, discharge voltage and pulse on time [25]. The EDM of ceramic composite was successful to machine complex shapes, but there were numerous drawbacks. Ceramic component machined by EDM showed an uneven fusing structure, globules of debris, shallow craters, micro-pores, micro-cracks and pockmarks which raised the demand of finishing processes after EDM of components [10].

One of the main hindrances to the full utilization of the potential of conductive ceramics is the non-availability of cost-effective machining method. The machining method used for machining of ceramics should not affect the physical and mechanical properties of the work material adversely. The diamond grinding of alumina ceramic was recently successful [13, 14]. The high grinding forces, surface and subsurface cracks, voids and pits were observed during alumina ceramic machining. It was observed that the ductile-mode grinding (grain dislodgement) was dominated by active grains, active grain protrusion angle, wheel speed and table speed, but it did not depend on the depth of cut which was assumed to be less than the grain protrusion height [26]. The process was mainly used for finishing therefore the MRR was very less and it involved high man machine time. Therefore, the processing of alumina ceramic by hybrid machining processes may be a better alternative.

The material removal mechanism in electrical discharge diamond grinding (EDDG) was studied by Koshy et al. and it was found that the discharges thermally softened the work material in grinding zone and the normal force and the grinding power were decreased [27-29]. The improved grinding performance was found due to continuous, in-process dressing and declogging of the wheel surface [30]. It was found that the use of a rotating disk electrode with effective flushing of the working gap was more productive and accurate technique and remarkably improved surface finish than the use of a conventional electrode [30, 31]. Koshy et al. studied the machinability of cemented carbide using EDDG. They found that the discharges improved the grinding performance by effectively declogging the wheel surface. The protrusion height was found uniformly distributed and the percentage of area due to exposed abrasives were independent of the abrasive grit size for a particular concentration [29, 32]. The increase in wear resistance was due to high fracture toughness of the material at high discharge currents. The influences of process parameters such as pulse current, duty ratio, wheel speed and grain size for the prediction of wheel wear and surface

roughness [33, 34]. It was concluded that the MRR reduced if the recast layer solidified prior to the non-conductive ceramic particle grinding [35].

The literature presented above indicated that the diamond grinding, EDM and EDDG processes were employed to machine ceramic composites. The alumina ceramic composite is of keen interest due to its increasing application in cutting tools, hip implants, dental implants, armours and die applications [1-8]. Although there were numerous attempts in the field of  $Al_2O_3-SiC_w-TiC$  ceramic processing, the efficient and cost effective processing method is still a challenge. At present, various efficacious hybrid machining processes are available like electrochemical arc machining (ECAM), electrochemical discharge machining (ECDM), ultrasonic assisted electric discharge machining (USEDM), electro chemical grinding (ECG) and electric discharge grinding (EDG) etc. The EDG process utilized benefits of EDM and conventional diamond grinding processes. In EDG, material is removed by grinding of softened work material and partially by melting and vaporization due to sparks. In case of non-homogeneous materials, despite of the hardness, toughness and brittleness, finished surface may be free from burrs or grinding burn marks. Therefore, the process like EDG may be more suitable than grinding or EDM processes alone for machining of  $Al_2O_3-SiC_w-TiC$ . In this work, an attempt has been made to study the influence of EDG process factors on responses like MRR and SR while machining of  $Al_2O_3-SiC_w-TiC$ . SEM micrographs of electric discharge grounded surfaces have been used for detailed study of surface/subsurface damages with respect to associated process factors.

#### Experimental procedure and analysis of experimental data

The EDG setup designed and fabricated by various researchers [31, 34, 36-38], has single support for the rotating grinding wheel, which may lead to high vibrations during the process. There was also possibility of axial misalignment due to grinding forces during processing of  $Al_2O_3-SiC_w-TiC$ . To overcome such problems few modifications in the setup were incorporated. The following section discusses the modification incorporated in the present setup used for EDG processing.

#### Setup design and fabrication

To perform the EDG experiments on "Electronica leader ZNC" die-sinking EDM machine, EDG set up was fabricated with few improvements in support and motion control. Two parallel plate were used to facilitate better support. These helped in proper holding of the wheel axis and maintain the parallelism with the work surface/table bed. The self-aligning cylindrical roller bearings were used to minimize the run-out and axial misalignment as shown in schematic diagram of the setup (figure 1).

Table 1 Physical and mechanical properties of  $Al_2O_3-SiC_w-TiC$  ceramic composite[10]

Hardness (H <sub>v</sub> )	Fracture toughness (MPa(m) <sup>0.5</sup> )	Thermal conductivity k(W/mK at 400°K)	Electrical Resistivity (Ωcm)	Density ρ (g/cm <sup>3</sup> )
2400	9.6±0.6	63	0.009	3.915

The precision and accuracy of the motion was maintained by using servo motors for rotation of grinding wheel and table in horizontal directions, as shown in figure 2. These servo motors were connected to a dedicated system through break out box and ACR processor-based 4 axis motion controllers. Aries view software has been used for ACR's processor-based 4 axis motion controllers.

**Sample preparation**

The electrically conductive  $Al_2O_3-SiC_w-TiC$  ceramic composite supplied by Industrial Ceramic Technology has been selected as workpiece. The ceramic composite was fabricated (by supplier) by ball milling the mixture of 46.1 vol. %  $Al_2O_3$  powder, 30.9 vol. %  $SiC$  whiskers and 23.0 vol. %  $TiC$  powder as presented in figure 3 [10]. The physical and mechanical

properties of the  $Al_2O_3-SiC_w-TiC$  ceramic composite have been summarized in table 1 [10]. The optical image of  $Al_2O_3-SiC_w-TiC$  composite has been shown in figure 4, where the bright grains are  $TiC$  particles, the light-grey particles are the  $SiC_w$ , and the dark-grey background is of alumina matrix [10]. The size of the workpiece considered in this work was a square of  $20 \times 20 \text{ mm}^2$  having uniform thickness of 5 mm. The work pieces were grounded by diamond grinding wheel of 200 mesh size, to achieve uniform average surface roughness in the range of 0.28 to  $0.30 \mu\text{m}$  before experimentation. In table 2, the process parameters have been summarized which were kept constant throughout experimentation. The specimen was cleaned in the acetone bath before taking surface roughness and weight loss measurements. Prior to experimentation dressing of the wheel was done to get uniform grain protrusion height and active edges along the grinding wheel surface.

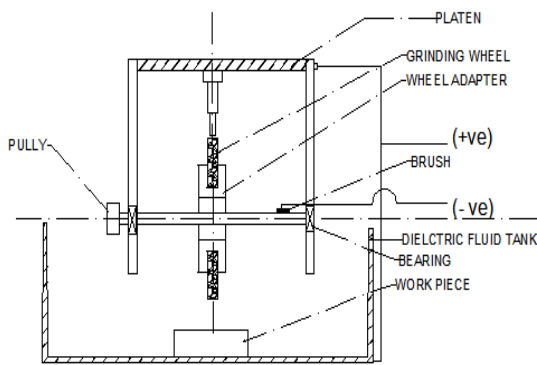


Figure 1 Schematical representation of experimental setup



Figure 2 Attached EDG setup on EDM machine

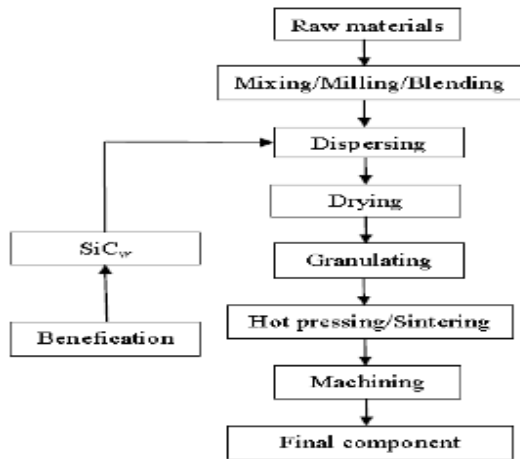


Figure 3 Processing steps in manufacturing of  $Al_2O_3-SiC_w-TiC$  composite [10]

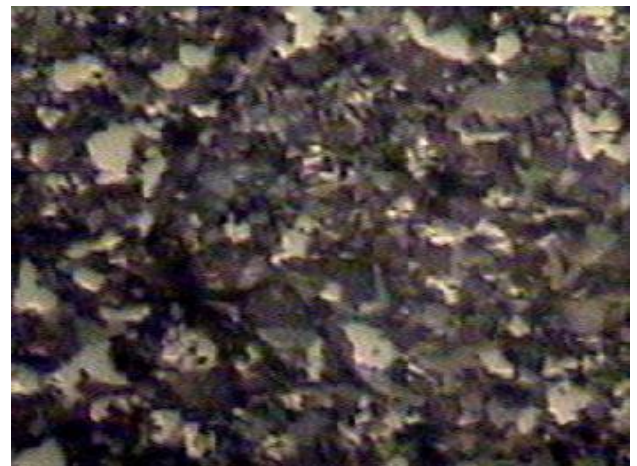


Figure 4 The optical micrograph of  $Al_2O_3-SiC_w-TiC$  composite

Table 2 Grinding wheel specifications and constant parameters in EDG processing

Grinding wheel specification		Duty ratio	0.56
Wheel diameter	100mm	Wheel speed	5m/s
Wheel bonding	Bronze	Parameters for EDG processing	
Abrasive grit size	#800 mesh	Polarity of wheel	Negative
Wheel thickness	20mm	Gap voltage for servo control	70V
Parameters for dressing of grinding wheel		Dielectric flushing	0.6MPa
Pulse peak current	10A	Dielectric	Kerosene
Pulse on time	200µs		

*Selection of process parameters*

Even though the performance of EDG process is governed by numerous interactive parameters of EDM and grinding processes, important process parameters of both processes were considered. Pilot experiments were carried out by one

variable at a time to determine the range of process factors. The range of process parameters determined has been presented in table 3. The machining time of 20 minute was suitably decided. Kerosene oil was used as dielectric medium.

Table 3 Coded levels of variables to the corresponding actual levels of variables

Process factors	Symbol	Coded variable levels				
		Lowest -2	Low -1	Centre 0	High +1	Highest +2
Discharge current (A)	$I_p$	3	4	5	6	7
Duty-ratio	$D_c$	0.24	0.40	0.56	0.72	0.88
Pulse on time (µs)	$T_{on}$	100	200	300	400	500
Table speed (m/min)	$V_t$	0.030	0.045	0.060	0.075	0.090
Wheel speed (m/min)	$V_w$	0.79	1.57	2.36	3.14	3.93

*Planning of experiments*

EDG experiments were performed on “Electronica leader ZNC” die-sinking EDM machine with attached EDG set up. The central composite rotatable design (CCRD) was chosen since it requires fewer numbers of experiments. Discharge current, duty-cycle, pulse on time, table speed and wheel speed were selected as process factors. The measurement of surface roughness was carried out on “Talysurf 6, Rank Taylor Hobson, England”. A traverse length of 2 mm with a cut-off evaluation length of 0.8 mm was selected. Five different locations on the surface were selected for roughness measurement. The average of 5 readings of average surface roughness values was considered. The weight measurement was carried out on “METTLER TOLEDO AB265-S/FACT” weighing machine with least count of 0.01mg. The experimental findings of MRR and SR with respect to trials are given in table 4. The surface damage was observed and characterised by using a Scanning Electron Microscope (SEM) EVO 50.

*Data analysis*

The data has been analysed by standard statistical tool known as analysis of variance (ANOVA). The significance of the process factors and its interactions was checked. The ANOVA was again carried out with the dropped insignificant terms and its interactions. The *F-ratio* of the developed model for a 95% confidence level was calculated, and was found greater than tabulated *F-ratio* which showed that the model was adequate. The *F-ratio* for lack of fit was found less than tabulated *F-ratio* at 95% confidence level. The ANOVA table for MRR after dropping insignificant terms has been presented in table 5. Here, it is important to mention that the interaction of discharge current has little significance, but the discharge current alone is insignificant. From table 5, the value of  $R^2$  was 98%, at the significance level of  $\alpha = 0.01$ , which showed that the developed model provided the strong correlation between process parameters and its interactions. The regression equation for MRR has been given below by equation (1).

$$\begin{aligned}
 \text{MRR} = & 0.00329647 - 0.00154184I_p + 0.000493847D_c + 0.000024T_{on} + 0.000023V_t + 0.000164I_p^2 \\
 & - 0.000026D_c^2 - 0.000000T_{on}^2 + 0.000067I_pD_c - 0.000002I_pT_{on} - 0.000005D_cV_t \\
 & - 0.000002T_{on}V_w + 0.000017V_tV_w
 \end{aligned} \tag{1}$$

Table 4 Measured responses corresponding to each experimental run

Run	$I_p$ (A)	$D_c$	$T_{on}$ ( $\mu s$ )	$V_t$ (m/min)	$V_w$ (m/min)	MRR (mg/min)	$R_a$ ( $\mu m$ )
1	4	0.40	400	0.075	3.14	9.43	0.4064
2	4	0.40	200	0.045	3.14	6.93	0.3285
3	5	0.56	300	0.060	2.36	8.52	0.2632
4	6	0.40	200	0.075	3.14	8.83	0.2851
5	4	0.72	200	0.045	1.57	7.01	0.0951
6	7	0.56	300	0.060	2.36	9.06	0.7166
7	6	0.72	400	0.075	3.14	9.76	1.0082
8	6	0.72	400	0.045	1.57	8.85	1.2919
9	5	0.56	300	0.030	2.36	7.42	0.1634
10	4	0.40	200	0.075	1.57	7.46	0.1807
11	5	0.56	100	0.060	2.36	6.98	0.0732
12	5	0.56	300	0.060	2.36	8.41	0.2305
13	6	0.40	400	0.045	3.14	7.54	0.5744
14	5	0.56	300	0.060	2.36	8.25	0.2489
15	5	0.56	300	0.060	3.93	8.91	0.6337
16	5	0.56	500	0.060	2.36	8.94	0.6837
17	6	0.72	200	0.075	1.57	8.06	0.4098
18	5	0.56	300	0.060	2.36	8.48	0.0624
19	5	0.88	300	0.060	2.36	8.68	0.8448
20	4	0.72	400	0.045	3.14	8.81	0.4872
21	3	0.56	300	0.060	2.36	8.99	0.4226
22	4	0.56	200	0.075	3.14	8.83	0.5105
23	6	0.72	200	0.045	3.14	8.53	0.4418
24	5	0.56	300	0.060	2.36	8.36	0.2567
25	6	0.40	400	0.075	1.57	8.25	0.4682
26	6	0.40	200	0.045	1.57	6.58	0.0993
27	4	0.40	400	0.045	1.57	8.09	0.2853
28	5	0.56	300	0.090	2.36	8.98	0.1124
29	5	0.24	300	0.060	2.36	7.23	0.3807
30	4	0.72	400	0.075	1.57	9.13	0.4298
31	5	0.56	300	0.060	0.79	7.56	0.0843
32	5	0.56	300	0.060	2.36	8.43	0.2475

The analysis of variance (ANOVA) was conducted for surface roughness ( $R_a$ ) as shown in table 6. The *F-ratio* of the developed model for a specific confidence level was calculated, and found greater than tabulated *F-ratio* at 95% confidence level and the model was found adequate. The *F-ratio* for lack of fit was found less than tabulated *F-ratio* at

95% confidence level, thus the lack of fit was insignificant. The value of  $R^2$  was 99.88%, at the significance level of  $\alpha = 0.01$ , which showed strong correlation among the input process parameters and its interactions. The regression equation for  $R_a$  has been given by equation (2).

$$\begin{aligned}
 R_a = & 3.65276 - 0.623437I_p - 0.528304D_c - 0.00621239T_{on} + 0.0204194V_t - 0.341095V_w + 0.0544I_p^2 \\
 & + 0.0224435D_c^2 + 0.000003869T_{on}^2 - 0.00014528V_t^2 + 0.129463V_w^2 + 0.0347813I_pD_c \\
 & + 0.00095175I_pT_{on} - 0.00273917I_pV_t - 0.0693159I_pV_w + 0.000340375D_cT_{on} \\
 & + 0.000332083D_cV_t - 0.00993523D_cV_w - 0.0000157T_{on}V_t - 0.0003389773T_{on}V_w \\
 & + 0.0050453V_tV_w
 \end{aligned} \tag{2}$$

Further, due to experimental error and noise present in the system, the value of estimated parameters and the responses like MRR and  $R_a$ , are subjected to uncertainty. Therefore, the

confidence interval was calculated to estimate the precision of MRR and  $R_a$  and is given by equation (3).

$$\Delta(\text{MRR or } R_a) = t_{\alpha/2, DF} \sqrt{V_e} \tag{3}$$

Table 5 Analysis of variance for MRR after reduction of insignificant terms

Source	DF	Seq SS	Adj SS	Adj MS	F	P
Regression	12	0.0000196	0.0000196	0.0000196	90.847	0.000000
Residual Error	19	0.0000003	0.0000003	0.0000000		
Lack-of-Fit	14	0.0000003	0.0000003	0.0000000	2.405	0.169969
Pure Error	5	0.0000000	0.0000000	0.0000000		
Total	31	0.0000199				

R-Sq = 98.29%                      R-Sq(pred) = 95.20%                      R-Sq(adj) = 97.21%

$F_{\text{Model}} > F_{0.01,12,19}$  Model is adequate ( $F_{0.01,12,19} = 3.80$ )                       $F_{\text{Lack of fit}} < F_{0.01,14,19}$  Lack of fit is insignificant ( $F_{0.01,14,19} = 3.51$ )

Table 6 Analysis of variance for SR after reduction of insignificant terms

Source	DF	Seq SS	Adj SS	Adj MS	F	P
Regression	19	2.12468	2.12468	0.111825	548.23	0.000000
Residual Error	12	0.00245	0.00245	0.000204		
Lack-of-Fit	7	0.00180	0.00180	0.000258	2.00	0.231723
Pure Error	5	0.00064	0.00064	0.000129		
Total	31	2.12713				

R-Sq = 99.88%                      R-Sq(pred) = 99.33%                      R-Sq(adj) = 99.70%

$F > F_{0.01,19,12}$  Model is adequate ( $F_{0.01,19,12} = 3.77$ )                       $F_{\text{Lack of fit}} < F_{0.01,7,12}$  Lack of fit is insignificant ( $F_{0.01,7,12} = 4.64$ )

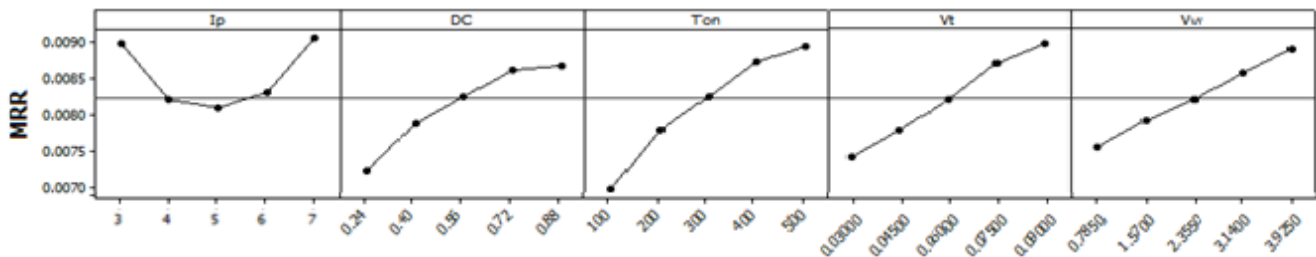


Figure 5 Main effect plot for material removal rate during EDG process

DISCUSSION

This section includes detailed discussion on the outcome of data analysis with respect to material removal rate, surface roughness and surface integrity of  $Al_2O_3-SiC_w-TiC$  composite processed by EDG. The percentage contribution of process factors and interactions have also been presented and discussed in this section. The response surfaces have been presented and the trends are explained in order to have a feel of associated process physics of material removal and surface generation in EDG process.

MATERIAL REMOVAL RATE

The main effect plot and the percentage contribution of various process factors and interactions with respect to MRR have been shown in figures 5 and 6 respectively. It can be seen from figure 5 that the MRR first decreases with the increase in discharge current upto 5A and then it increases, however figure 6 shows that that the influence of discharge current is insignificant as compared to its interaction.

Figure 5 indicates that the increase in duty cycle and pulse on time increases the MRR. The increase in pulse on time or duty cycle increases the discharge energy per spark and hence a large size crater is formed on workpiece resulting in higher MRR [39]. The increase in table speed and wheel speed also increases the MRR as shown in figure 5. The increase in table speed causes availability of more uncut material per unit time available for abrasives to cut and increase in grinding wheel speed causes more number of abrasives per unit time which can engage with the available workpiece material and causes increase in MRR. The observed trend of discharge current, duty cycle, pulse on time, wheel speed and table speed are similar to the trends predicted by mathematical model for MRR by EDG process [39, 40]. The interaction terms having contribution of less than 5% (figure 5) are considered to be insignificant, but these cannot be excluded from the model as exclusion of these terms results in inadequacy of the model and significant lack of fit.

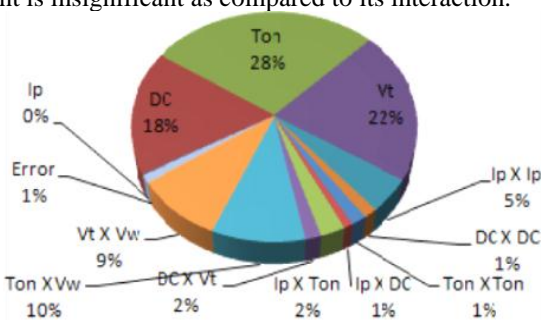


Figure 6 Percentage contribution of process factors and interactions on MRR

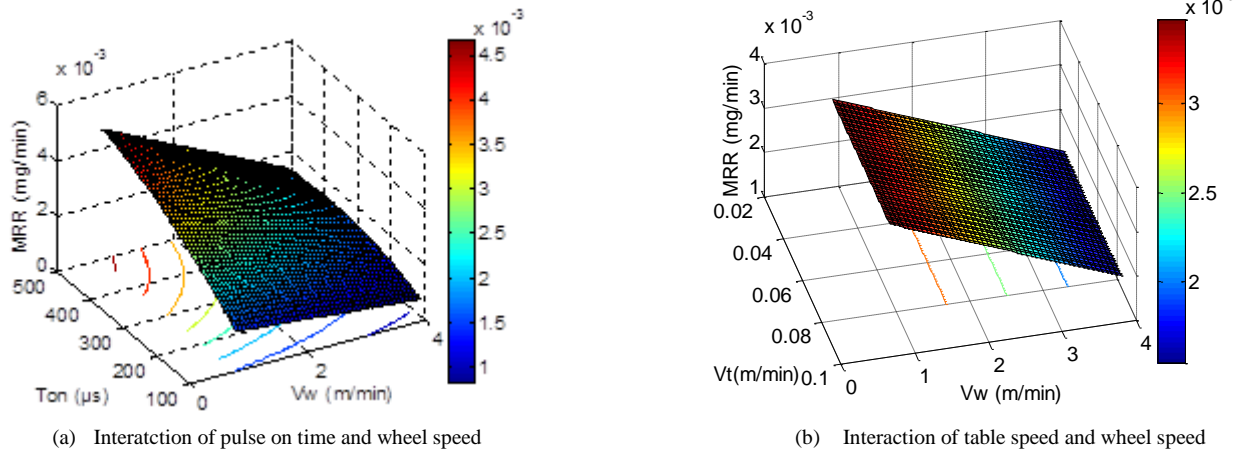


Figure 7 Response surface plots of the significant interaction terms for MRR

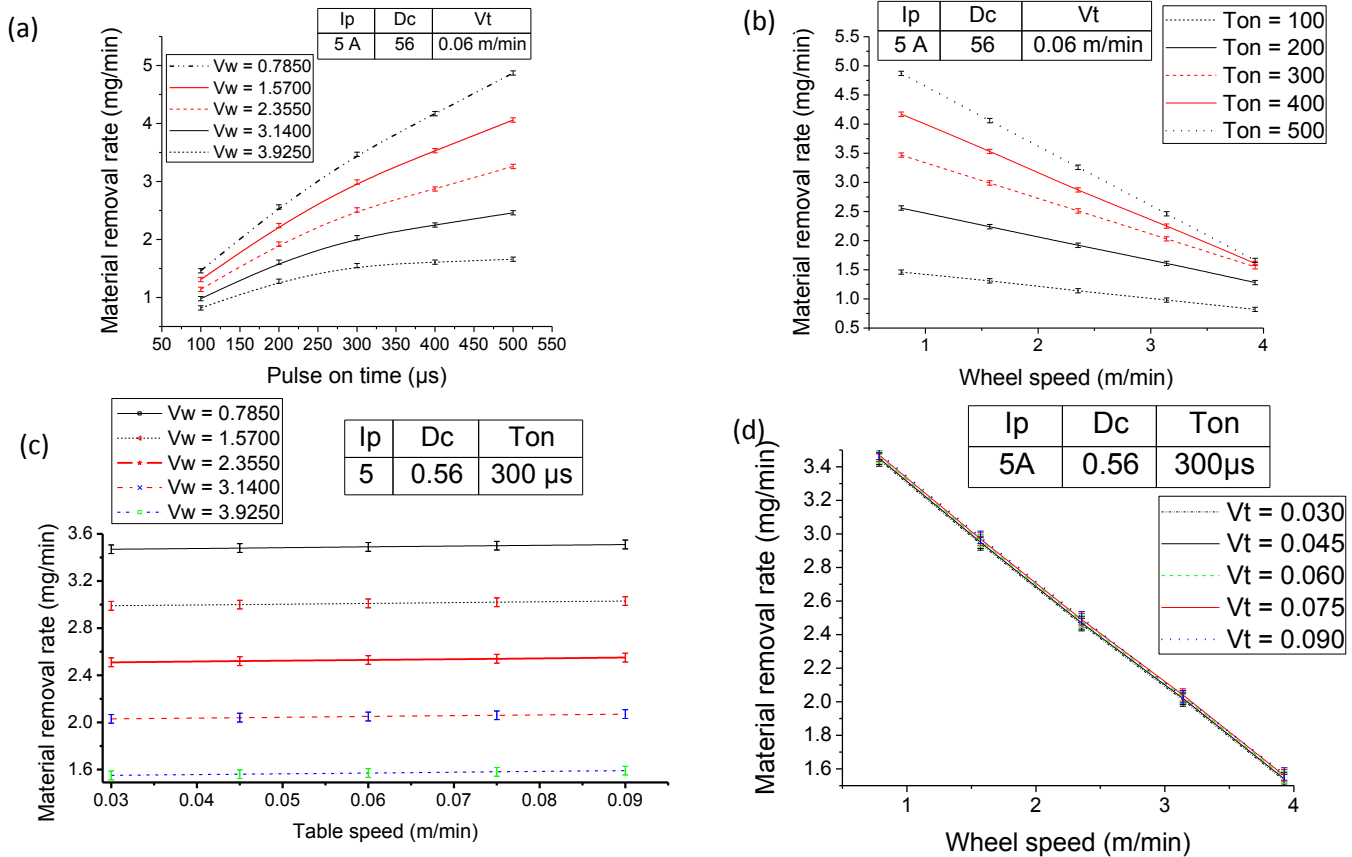


Figure 8 Variation of MRR with respect to significant process factors related to interactions for MRR

The response surfaces showing the effect of significant interaction terms (>5%) affecting MRR have been presented in figure 7 and 8. Figure 7(a) and figures 8 (a-b) shows the interaction of pulse on time and grinding wheel speed. It shows that the increase in pulse on time increases the MRR, whereas the increase in wheel speed reduces the MRR. The increase in MRR with the increase in pulse on time may be due to the increase in discharge energy. The increase in discharge energy causes formation of a bigger size crater on the work surface and hence leads to the increase in MRR. At the same time, when wheel speed is increased along with increase in pulse on time, it causes reduction in MRR which may be due to the reason that high energy discharge causes a larger crater and thus unavailability of material that might

have been removed as much number of grits passes the work surface due to high wheel speed.

Figure 7(b) and figures 8(c-d) shows the interaction of table speed and wheel speed. The increase in table speed does not influence the MRR, whereas the simultaneous increase in wheel speed reduces the MRR. The increase in table speed raises the feed rate of work material promoting ductile mode grinding which is dominated by the number of active grits [26], but due to constant wheel speed the influence of feed is negligible. Whereas, the table speed alone result's in increased material removal rate. The similar trend has been reported by Satyarthi and Pandey for effect of table speed alone on MRR [39]. The simultaneous increase in wheel speed shows reduction in MRR as at high wheel and tables speeds the ductile work-material loads the grinding wheel

and wheel may lose its cutting ability resulting in reduction in MRR, the result are in agreement of the findings of singh et al. [41].

**Surface roughness**

The main effect plot and the percentage contribution of various process factors and interactions with respect to surface roughness (SR) have been shown in figure 9 and 10 respectively. Figure 9 shows that the SR increases with the increase in discharge current, duty cycle and pulse on time, which may be due to increased discharge energy resulting in large size craters. The increase in table speed upto 0.06m/min

increases the SR but further increase in table speed, results in reduced SR. Similarly the increase in wheel speed upto 1.57m/min reduces the SR but further increase in wheel speed results in increased SR. However, figure 10 shows that the influence of table speed and wheel speed is insignificant (2% and 0% respectively) as compared to its interactions. The interaction terms having contribution of less than 5% (figure 10) are considered to be insignificant, but these cannot be excluded from the model as exclusion of these terms results in inadequacy of the model and significant lack of fit.

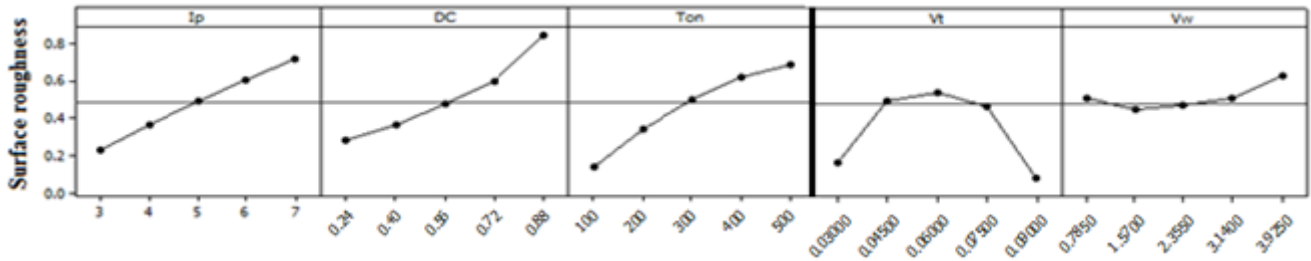


Figure 9 Main effect plot for surface roughness during EDG process

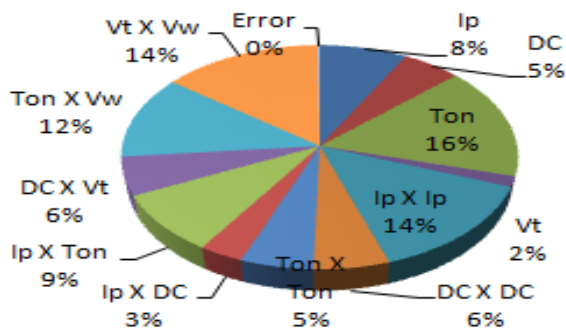


Figure 10 Percentage contributions of factors and interactions on surface roughness

The response surfaces showing the effect of significant interaction terms (>5%) affecting SR have been presented in figure 11 and 12. Figure 11(a) and figures 12(a-b) show the interaction of discharge current and pulse on time. The figures show that when discharge current is increased and pulse on time is kept at lower side the surface roughness decreased with the increase in discharge current.

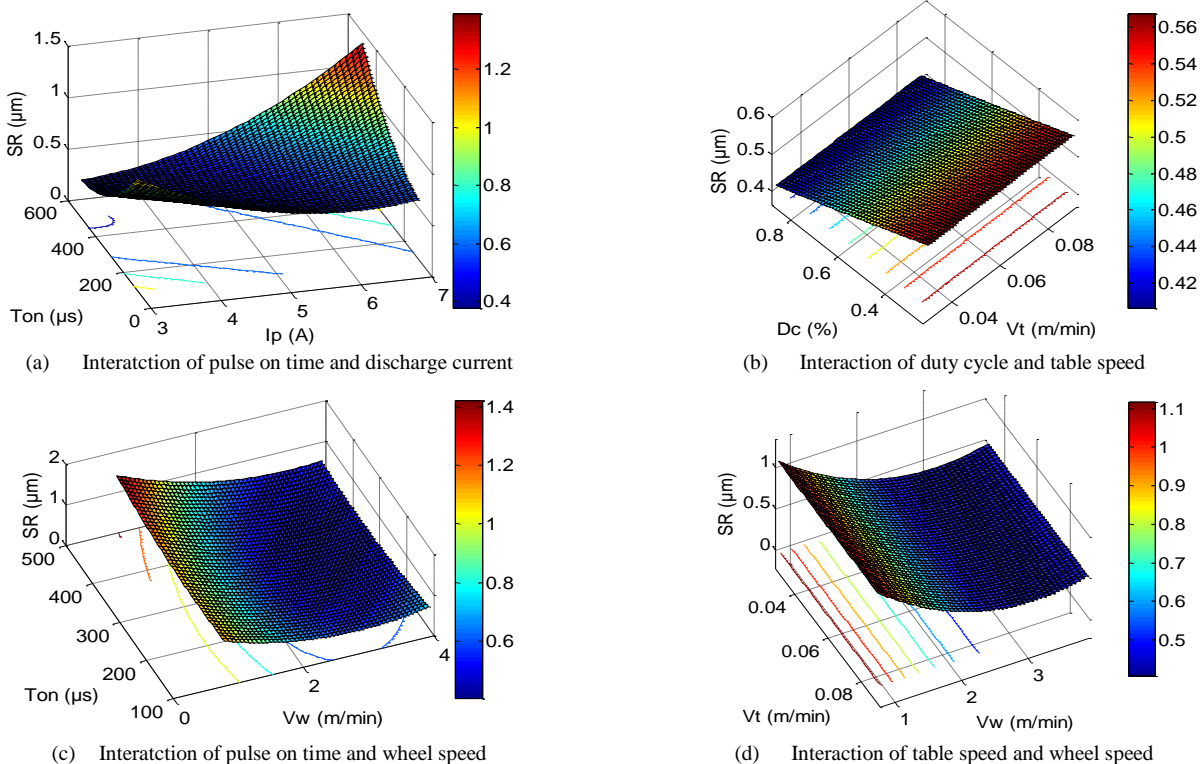


Figure 11 Response surface plots of the significant interaction terms for SR



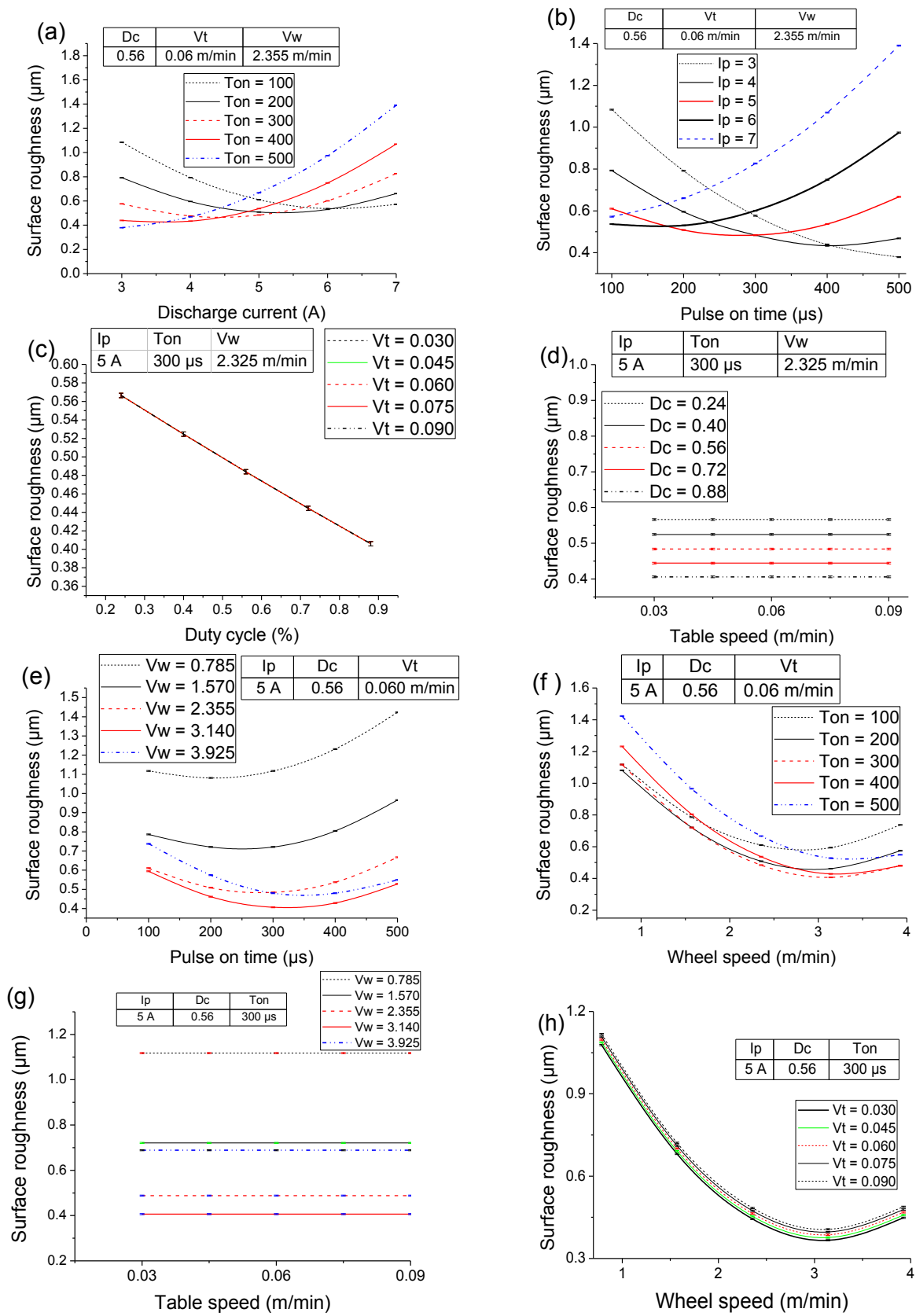


Figure 12 Plots of process parameter corresponding to response surface (figure 11)

It can be seen from figure 10 that the pulse on time affects the process more than the discharge current as the percentage contribution of discharge current is lower than

the percentage contribution of pulse on time. Therefore when pulse on time is low and discharge current is increased the size of craters which are formed are such that

these craters are being filled due to sweeping of molten material of by the grinding action and improvement in surface quality is obtained. However when the pulse on time is long and the discharge current is increased there is increase in SR. As the pulse on time dominates discharge current (as indicated by figure 10) very large size craters may form and the grinding action is unable to completely fill and improve the surface quality due to larger depths. Figure 11(b) and figures 12(c-d), shows that the increase in duty cycle reduces the SR and the effect of table speed is negligible. The increase in duty cycle results in reduced pulse off time as the pulse on time is kept constant, which shows that the sparking takes place after small interval of time. Because the work table keeps moving, the spark location is likely to be closer to each other with increase in duty cycle (when pulse on time is kept constant). If these spark locations are such that their some portion overlaps and the molten material is being swept by the grinding action, it may result into smoother surface and hence the surface roughness decreases. Figure 11(c) and figures 12(e-f), show that the surface roughness reduces with increase in grinding wheel speed up to certain limit and then it increases. This trend conforms to the physics of grinding as

in grinding process [42, 43]. However with increase in pulse on time the surface roughness reduces upto a limit and then it increases. This may be due to the size of the craters formed at different pulse on times and the three situations of interactions of abrasive grits [39].

Figure 11(d) and figures 12(g-h), show the interaction effect of table speed and wheel speed. Although, the influence of table speed and wheel speed alone were insignificant i.e. 2% and 0% respectively, but the interaction of table speed with wheel speed plays prominent role with respect to the SR. The increase in table speed does not influence the SR, however the increase in wheel speed first reduces the SR upto a limit and then it increases. This trend confirms the physics of grinding [42, 43]. The increase in wheel speed results into the interaction of more number of abrasive grits per unit time, with the molten material due to formation of craters and causes improved sweeping and smoother surface, but when the wheel speed is increased beyond a limit it results in increased SR due to wheel loading which may take place due to increased temperature in the grinding zone because of very high speed grinding.

Table 7 Optimum process parameters

<i>EDG Response</i>	$I_p$ (A)	$D_c$ (%)	$T_{on}$ ( $\mu s$ )	$V_t$ (m/min)	$V_w$ (m/min)	Calculated optimum	Experimental value
$MRR_{max}$	7	0.88	500	0.030	3.93	9.91 (mg/min)	9.88 (mg/min)
$Ra_{min}$	3	0.24	100	0.030	3.93	0.0612 ( $\mu m$ )	0.0609 ( $\mu m$ )

*Process optimization*

In present work an attempt has been made to estimate processing conditions for highest possible MRR and lowest possible SR. To achieve this, optimization of the equations (1) and (2) has been done by a standard MATLAB 2011a

function, *fmincon* [44], which can handle optimization problems of the nonlinear nature. The obtained optimization results have been validated by conducting experiments are presented in table 7.

*Surface topography*

The outcome of data analysis and its discussion in previous sections revealed that the EDG process is governed prominently by discharge energy and grinding action. The discharge energy is a function of discharge current and pulse on time/duty cycle. The increase in discharge current and pulse on time increases the discharge energy. Increase in duty cycle reduces the pulse off time and pulse on time increases, which contributes in increase of discharge energy. The amount of discharge energy transferred from tool to workpiece and simultaneous grinding action give rise to either of the three conditions as discussed below [39]. Figure 13 shows the scanning electron micrographs obtained when workpiece is acted with low discharge energies, and the grinding action remains prominent and the material is removed by the abrasion. The higher penetration of the grits may be witnessed by the presence of grinding marks on the work surface as shown in figure 13(a). The material being brittle in nature promotes brittle regime fracture (grain dislodgement) as shown in figure 13(b). The high MRR with considerably high surface roughness may be attributed to ploughing action of grinding.

Figures 14 shows the scanning electron micrographs when work surface is exposed to higher discharge energy leading to thermal softening of work material along with very efficient abrasion by abrasive grits due to grinding action. The improvement in MRR and surface finish is therefore observed. The surfaces shown in the figure is free from surface and sub-surface damages. The recast layer might have been swept completely by the grinding action.

Figure 15 shows the third condition that is when discharge energy is increased even more and the EDM action becomes prominent. The bigger size craters of high depths are formed due to increased discharge energy and are partially filled by molten material. The grinding action in the case is unable to remove the complete molten material due high depths of craters and this is being swept uniformly as recast layer of uniform thickness has been found on the machined work surfaces as shown in figure 15(b). In this case the reduced MRR was attributed to the formation of bigger size craters which nullifies the contribution of grinding action for MRR during the EDG process.

It can be seen from figures 13–15 that EDG processed workpieces are generally free from surfaces and subsurface damages and defects like pits, burn marks and heat affected zone (HAZ) this is in agreement to the findings [34]. Grain

dislodgement and deposited recast layer were few drawbacks at low and high discharge energy conditions. Figure 14 shows work surface of least surface roughness (0.0624 $\mu$ m) obtained by EDG process. The achieved surface roughness in the present work is lesser than the reported surface roughness's obtained when alumina  $Al_2O_3$ -SiCw-TiC composite is processed by EDM or conventional diamond grinding [18, 19] the results are in agreement to the work done on ED milling in combination with mechanical grinding

[45]. The MRR obtained by EDG process was found to be 4 to 10 times higher than the EDM. The surface roughness achieved by EDG was 2 to 5 times lower than EDM. It was also found that the surface topography obtained by EDG process was better than EDM and conventional diamond grinding processes [19]. The surface and subsurface defects induced by EDM and grinding processes alone are not observed when  $Al_2O_3$ -SiCw-TiC composite is processed by their hybrid process EDG.

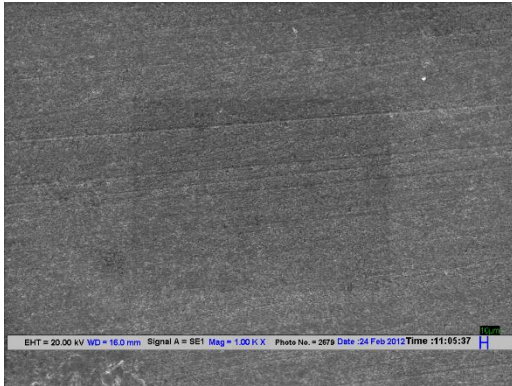


Figure 13 (a) SEM showing surface texture after EDG at Ip-3, DC-0.56, Ton-300, Vt-0.06 and Vw-2.36

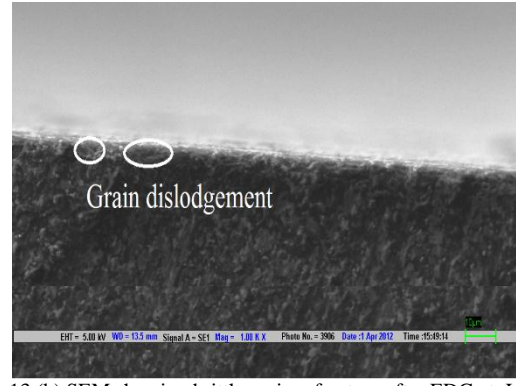


Figure 13 (b) SEM showing brittle regime fracture after EDG at Ip-3, DC-0.56, Ton-300, Vt-0.06 and Vw-2.36

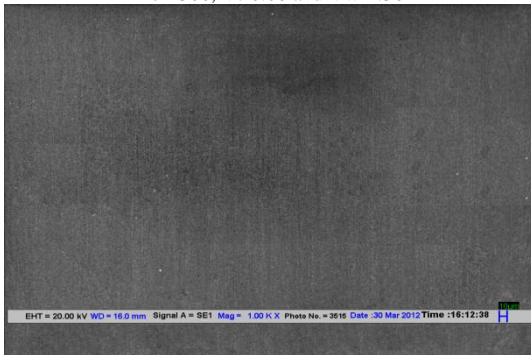


Figure 14 (a) SEM showing surface texture after EDG at Ip-4, DC-0.40, Ton-300, Vt-0.06 and Vw-2.36

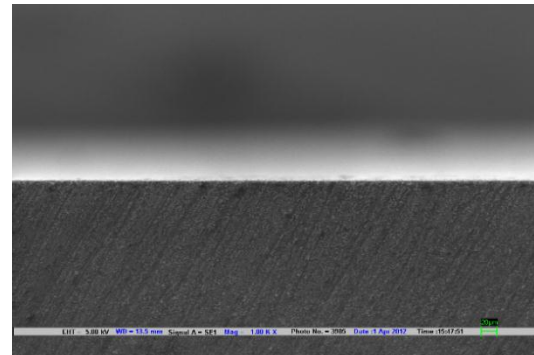


Figure 14 (b) SEM showing surface texture after EDG at Ip-4, DC-0.40, Ton-300, Vt-0.06 and Vw-2.36

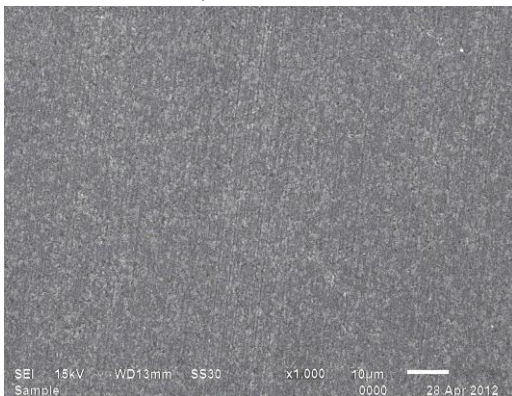


Figure 15 (a) SEM showing surface texture after EDG at Ip-5, DC-0.56, Ton-500, Vt-0.045 and Vw-3.93

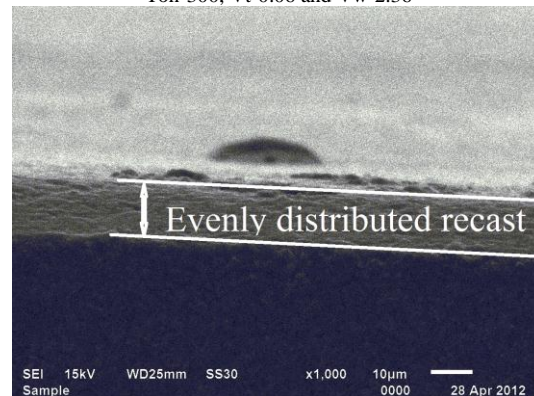


Figure 15 (b) SEM showing uniformly swept recast layer after EDG at Ip-5, DC-0.56, Ton-500, Vt-0.045 and Vw-3.93

### CONCLUSIONS

In the present work machining of  $Al_2O_3$ -SiCw-TiC has been successful performed on the developed EDG setup. The results indicated that the discharge current alone did not influence the MRR significantly, but the interaction of discharge current with duty cycle, pulse on time, table speed and wheel speed played prominent role. The highest MRR

obtained by EDG was 9.76 mg/min. The results also indicated that the wheel speed and table speed alone did not influence the surface roughness significantly, but the interaction of wheel speed with discharge current, duty cycle, pulse on time and table speed played prominent role. The least average surface roughness obtained by EDG process was 62 nm. The defects induced by EDM and conventional

diamond grinding processes were not observed on EDG processed surfaces. Although, recast layer was observed in few cases which was swept uniformly along the work surface resulting in lower SR.

#### ACKNOWLEDGEMENTS

The authors would like to thank Mr. John J. Schuldies, President, Industrial Ceramic Technology Inc, Ann Arbor

Michigan, USA, for supplying electrically conductive  $Al_2O_3$ - $SiC_w$ - $TiC$  ceramic composite work material and relevant data. The authors would also like to acknowledge the financial support of Department of Science and Technology (DST) Delhi, India to carry out this work.

#### REFERENCES

- [1] Yeniyl, S., et al., *Relative Contributions of Surface Roughness and Crystalline Structure to the Biocompatibility of Titanium Nitride and Titanium Oxide Coatings Deposited by PVD and TPS Coatings*. ISRN Biomaterials, 2013. 2013: p. 9.
- [2] Sugano, N., et al., *20-Year Survival of Cemented Versus Cementless Total Hip Arthroplasty for 60-Year Old or Younger Patients With Hip Dysplasia*. Bone & Joint Journal Orthopaedic Proceedings Supplement, 2013. 95-B(SUPP 15): p. 343-343.
- [3] Mohanty, S., A.P. Rameshbabu, and S. Dhara, *Net shape forming of green alumina via CNC machining using diamond embedded tool*. Ceramics International, 2013(Accepted manuscript).
- [4] Senthil Kumar, A., A. Raja Durai, and T. Sornakumar, *Development of alumina-ceria ceramic composite cutting tool*. International Journal of Refractory Metals and Hard Materials, 2004. 22(1): p. 17-20.
- [5] Sornakumar, T., et al., *Development of alumina and Ce-TTZ ceramic-ceramic composite (ZTA) cutting tool*. International Journal of Refractory Metals and Hard Materials, 1995. 13(6): p. 375-378.
- [6] Mendez-Vilas, A., *Fuelling the Future: Advances in Science and Technologies for Energy Generation, Transmission and Storage*. 2012: Universal-Publishers. 615.
- [7] Darolia, R., *Thermal barrier coatings technology: critical review, progress update, remaining challenges and prospects*. International Materials Reviews, 2013.
- [8] Azarafza, R., et al., *Impact Behavior of Ceramic-Metal Armour by  $Al_2O_3$ -Nano  $SiC$  Nano Composite*. International Journal of Advanced Design and Manufacturing Technology, 2013. 5(5): p. 83-87.
- [9] Anand Dev, et al., *Machining characteristics and optimisation of process parameters in micro-EDM of  $SiCp$ - $Al$  composites*. International Journal of Manufacturing Research, 2009. 4(4): p. 458-480.
- [10] Patel, K.M., P.M. Pandey, and P. Venkateswara Rao, *Surface integrity and material removal mechanisms associated with the EDM of  $Al_2O_3$  ceramic composite*. International Journal of Refractory Metals and Hard Materials, 2009. 27(5): p. 892-899.
- [11] Patel, K.M., P.M. Pandey, and P.V. Rao, *Determination of an Optimum Parametric Combination Using a Surface Roughness Prediction Model for EDM of  $Al_2O_3/SiC_w/TiC$  Ceramic Composite*. Materials and Manufacturing Processes, 2009. 24(6): p. 675-682.
- [12] Ramulu, M., G. Paul, and J. Patel, *EDM surface effects on the fatigue strength of a 15 vol%  $SiCp/Al$  metal matrix composite material*. Composite Structures, 2001. 54(1): p. 79-86.
- [13] Singh, V., S. Ghosh, and P.V. Rao, *Comparative Study of Specific Plowing Energy for Mild Steel and Composite Ceramics Using Single Grit Scratch Tests*. Materials and Manufacturing Processes, 2011. 26(2): p. 272-281.
- [14] Verma, V.K., V. Singh, and S. Ghosh, *Comparative grindability study of composite ceramic and conventional ceramic*. International Journal of Abrasive Technology 2010 3(3): p. 259 - 273.
- [15] Shih, H. and K. Shu, *A study of electrical discharge grinding using a rotary disk electrode*. The International Journal of Advanced Manufacturing Technology, 2008. 38(1-2): p. 59-67.
- [16] Jones, A.H., R.S. Dohedoe, and M.H. Lewis, *Mechanical properties and tribology of  $Si_3N_4$ - $TiB_2$  ceramic composites produced by hot pressing and hot isostatic pressing*. Journal of the European Ceramic Society, 2001. 21(7): p. 969-980.
- [17] Patel, M.R., et al., *Theoretical models of the electrical discharge machining process. II. The anode erosion model*. Journal of Applied Physics, 1989. 66(9): p. 4104-4111.
- [18] Satyarthi, M.K. and P.M. Pandey, *Processing of conductive ceramic composite by EDG and powder mixed EDG: A comparative study*. in *4th International and 25th All India Manufacturing Technology, Design and Research Conference (AIMTDR-2012)*. 2012. Jadavpur University, Kolkata, India.: EXCEL INDIA PUBLISHERS.
- [19] Satyarthi, M.K. and P.M. Pandey, *Comparison of EDG, Diamond Grinding, and EDM Processing of Conductive Alumina Ceramic Composite*. Materials and Manufacturing Processes, 2013. 28(4): p. 369-374.
- [20] Puertas, I. and C.J. Luis, *A Study of Optimization of Machining Parameters for Electrical Discharge Machining of Boron Carbide*. Materials and Manufacturing Processes, 2004. 19(6): p. 1041-1070.
- [21] Ramarao, P.V. and M.A. Faruqi, *Characteristics of the surfaces obtained in electro-discharge machining*. Precision Engineering, 1982. 4(2): p. 111-113.
- [22] Puertas, I. and C.J. Luis, *A study on the electrical discharge machining of conductive ceramics*. Journal of Materials Processing Technology, 2004. 153-154: p. 1033-1038.
- [23] Puertas, I. and C. Perez, *Modelling the manufacturing parameters in electrical discharge machining of siliconized silicon carbide*. Proceedings of the Institution of Mechanical Engineers, Part B: Journal of Engineering Manufacture, 2003. 217(6): p. 791-803.
- [24] Trueman, C.S. and J. Huddleston, *Material removal by spalling during EDM of ceramics*. Journal of the European Ceramic Society, 2000. 20(10): p. 1629-1635.
- [25] Ramasawmy, H., L. Blunt, and K.P. Rajurkar, *Investigation of the relationship between the white layer thickness and 3D surface texture parameters in the die sinking EDM process*. Precision Engineering, 2005. 29(4): p. 479-490.
- [26] Xie, J. and Y.X. Lu, *Study on axial-feed mirror finish grinding of hard and brittle materials in relation to micron-scale grain protrusion parameters*. International Journal of Machine Tools and Manufacture, 2011. 51(1): p. 84-93.
- [27] Koshy, P., V.K. Jain, and G.K. Lal, *Mechanism of material removal in electrical discharge diamond grinding*. International Journal of Machine Tools and Manufacture, 1996. 36(10): p. 1173-1185.
- [28] Jain, V.K. and R.G. Mote, *On the temperature and specific energy during electrodischarge diamond grinding (EDDG)*. International Journal of Advanced Manufacturing Technology, 2005. 26: p. 56-67.
- [29] Koshy, P., V.K. Jain, and G.K. Lal, *Grinding of cemented carbide with electrical spark assistance*. Journal of Materials Processing Technology, 1997. 72(1): p. 61-68.
- [30] Chattopadhyay, K.D., et al., *Analysis of rotary electrical discharge machining characteristics in reversal magnetic field for copper-en8 steel system*. International Journal of Advanced Manufacturing Technology, 2008. 38(9-10): p. 925-937.
- [31] Koshy, P., V.K. Jain, and G.K. Lal, *Experimental investigations into electrical discharge machining with a rotating disk electrode*. Precision Engineering, 1993. 15(1): p. 6-15.
- [32] Koshy, P., V.K. Jain, and G.K. Lal, *Stochastic simulation approach to modelling diamond wheel topography*. International Journal of Machine Tools and Manufacture, 1997. 37(6): p. 751-761.
- [33] Choudhury, S.K. and S. Kumar, *Prediction of wear and surface roughness in electro-discharge diamond grinding*. Journal of Materials Processing Technology, 2007. 191(1-3): p. 206-9.
- [34] Kumar Singh Yadav, S., V. Yadava, and V. Lakshmi Narayana, *Experimental study and parameter design of electro-discharge diamond grinding*. The International Journal of Advanced Manufacturing Technology, 2008. 36(1-2): p. 34-42.
- [35] Shu, K.M. and G.C. Tu, *Study of electrical discharge grinding using metal matrix composite electrodes*. International Journal of Machine Tools and Manufacture, 2003. 43(8): p. 845-854.
- [36] Kumar Singh Yadav, S., V. Yadava, and V. Lakshmi Narayana, *Experimental study and parameter design of electro-discharge diamond grinding*. International Journal of Advanced Manufacturing Technology, 2008. 36(1): p. 34-42.

- [37] Singh, G.K., V. Yadava, and R. Kumar, *Experimental study and parameter optimisation of electro-discharge diamond face grinding*. International Journal of Abrasive Technology, 2011. 4(1): p. 14-40.
- [38] Yadava, V., V.K. Jain, and P.M. Dixit, *Parametric study of temperature distribution in electrodischarge diamond grinding*. Materials and Manufacturing Processes, 2004. 19(6): p. 1071-101.
- [39] Satyarthi, M.K. and P.M. Pandey, *Modeling of material removal rate in electric discharge grinding process*. International Journal of Machine Tools and Manufacture, 2013. 74(0): p. 65-73.
- [40] Satyarthi, M.K. and P.M. Pandey, *Modeling of material removal rate in Electric Discharge Grinding process*. International Journal of Machine Tools and Manufacture, (Accepted Manuscript).
- [41] Singh, G.K., V. Yadava, and R. Kumar, *Diamond Face Grinding of WC-Co Composite with Spark Assistance: Experimental Study and Parameter Optimization*. International Journal of Precision Engineering and Manufacturing, 2010. 11(4): p. 509-18.
- [42] Yoshihara, N., T. Kuriyagawa, and K. Syoji, *Effect of Wheel Revolutionary Speed on Striped Pattern on Surfaces Finished by High-speed Reciprocation Grinding*, in *Initiatives of Precision Engineering at the Beginning of a Millennium*, I. Inasaki, Editor. 2002, Springer US. p. 446-450.
- [43] Groover, M.P., *Fundamentals of Modern Manufacturing: Materials, Processes, and Systems*. 2010: John Wiley & Sons.
- [44] Bacchewar, P.B., S.K. Singhal, and P.M. Pandey, *Statistical modelling and optimization of surface roughness in the selective laser sintering process*. Proceedings of the Institution of Mechanical Engineers, Part B: Journal of Engineering Manufacture, 2007. 221(1): p. 35-52.
- [45] Ji, R., et al., *Optimizing machining parameters of silicon carbide ceramics with ED milling and mechanical grinding combined process*. The International Journal of Advanced Manufacturing Technology, 2010. 51(1-4): p. 195-204.